ELSEVIER

Synthesis, biodistribution and excretion of radiolabeled poly(2-alkyl-2-oxazoline)s

Florian C. Gaertner [a,1], Robert Luxenhofer [b,1], Birgit Blechert [a], Rainer Jordan [b,*], Markus Essler [a,*]

[a] *Nuklearmedizinische Klinik und Poliklinik, Klinikum rechts der Isar, Technische Universität München, Ismaninger Str. 22, 81675 München, Germany*
[b] *Lehrstuhl für Makromolekulare Stoffe, Department Chemie, Technische Universität München, Lichtenbergstrasse 4, 85747 Garching, Germany*

Abstract

Here we report on the preparation of well defined water-soluble poly(2-methyl-2-oxazoline) and poly(2-ethyl-2-oxazoline) terminally equipped with a chelator (N,N′,N″,N‴-tetraazacylododecane-1,4,7,10-tetraacetic acid (DOTA)) for radionuclide labeling. The tissue distribution and excretion of ^{111}In-labeled poly(2-alkyl-2-oxazoline)s were studied in mice. We found that the hydrophilic polymers do not accumulate in tissues and are rapidly cleared from the blood pool, predominantly by glomerular filtration in the kidneys. In contrast only a small fraction is excreted via the hepatobiliary tract. Only minimal amounts of poly(2-alkyl-2-oxazoline)s are taken up by the reticuloendothelial system (RES). Scintigraphic studies revealed the feasibility of *in vivo* imaging of ^{111}In-labeled poly(2-oxazoline)s. Since additional functionalities for targeting can readily be introduced into poly(2-oxazoline)s via functional monomer units, these compounds fulfill fundamental requirements for an application as carrier molecules in radionuclide therapy.
© 2007 Elsevier B.V. All rights reserved.

Keywords: Poly(2-oxazoline); ^{111}In; DOTA; Biodistribution; Biocompatibility

1. Introduction

The development of tumor-specific targeting compounds is a central aim of modern oncology. A prerequisite for specific tumor targeting is the generation of appropriate carriers for anti-tumor drugs. Already in 1975 Ringsdorf [1] suggested a polymer-based carrier system which should be chemically well defined, water soluble and biocompatible. Compared to the use of low molar mass compounds the 'polymer approach' has various advantages as specificity and avidity of the drug conjugate can be easily modified. Multi-functional polymers for conjugation with several copies of targeting molecules, drugs or radionuclides can be synthesized in a single polymerization reaction, whereas multi-functional, low molar mass compounds typically require a multi-step reaction. Moreover, it was found that polymer-conjugates of cytotoxic drugs such as doxorubicin show dramatically reduced unspecific toxicity and improved bioavailability [2]. In this context, the conjugation of drugs to the hydrophilic poly(ethylene glycol) (PEG) is the most prominent example (PEGylation) [3]. PEG is synthesized via living anionic polymerization and is therefore highly defined in terms of targeted molar mass and molar mass distribution. However, the functionalization of PEG is limited to the two chain ends and multiple functionalization is only possible with branched or dendritic PEG derivatives [4,5].

A potential alternative to PEG is poly(2-oxazoline) (POx). Just like PEG, POx with a methyl- or ethyl-side chain are highly water-soluble and some conclusive studies report a good biocompatibility of this class of polymers [6]. Studies on POx grafted liposomes and micelles [7–9] did not report any adverse

---
* Corresponding authors. R. Jordan is to be contacted at Lehrstuhl für Makromolekulare Stoffe, Department Chemie, Technische Universität München, Lichtenbergstrasse 4, 85747 Garching, Germany. Tel.: +49 89 289 13581; fax: +49 89 289 13562. M. Essler, Nuklearmedizinische Klinik und Poliklinik, Klinikuh rechts der Isar, Technische Universität München, 81675 München, Germany. Tel.: +49 89 4140 2969; fax: +49 89 4140 4950.
  E-mail addresses: Rainer.Jordan@tum.de (R. Jordan), Markus.Essler@gmx.de (M. Essler).
[1] Both authors contributed in same parts to this article and are to be regarded as first authors.

effects of the polymer in animal models and suggest that POx behave similar to PEG for this type of conjugates (stealth liposomes). POx is synthesized via living cationic polymerization and can be synthesized with the same structural definition. Typically, the polydispersity (PDI) is low ($M_w/M_n \sim 1.2$) and the chain termini can be functionalized via the termination [10–16] or initiation method [10,11,17–22].

In contrast to PEG, POx can be easily equipped with side chain functionalities to modify the solubility (e.g. longer *n*-alkyl chains) or with chemical functions to allow coupling of targeting moieties such as peptidic motifs. Additional to the already existing functions such as hydroxyl- [23,24], phenyl- [25], carboxyl- [23,26], carbazol-functionalities [27,28], iodo-aryl- [29], bipyridyl- [30,31], as well as furan- and maleimide modifications [32], we introduced recently the aldehyde [33], alkyne [10] and amine [34] functionalities.

Despite their interesting characteristics and their chemical variability only one study about the biodistribution of POx *in vivo* has been published. Goddard et al. [6] reported on the synthesis and biodistribution studies of a radiolabeled poly[(2-methyl-2-oxazoline)-co-(2-(4-hydroxyphenyl)-2-oxazoline)] (PMOx-co-HphOx) polymer in mice. After injection, significant tracer accumulation was only found in samples of skin and muscle tissue. Especially, the low accumulation of the polymer in the reticuloendothelial system (RES), in liver and spleen would make POx a potential candidate for an application in radionuclide therapy.

However, the defined synthesis of the PMOx-co-HphOx copolymer seemed to be difficult and polymers with broad molar mass distributions were obtained, hence post polymerization fractionation had to be used to reduce the polydispersity of the polymer for biodistribution studies. This might be attributed to the 4-hydroxyphenyl-2-oxazoline comonomer which interferes with the living cationic polymerization (i.e. cross-linking, termination reaction). Thus, a more defined synthesis of radiolabeled hydrophilic POx is needed in order to investigate the biodistribution of this promising polymer class.

A first step to develop tumor-targeting devices with POx carriers could be the defined synthesis of POx-polymers conjugated with *N,N',N'',N'''*-tetraazacylododecane-1,4,7,10-tetraacetic acid (DOTA), a common chelator for various diagnostically or therapeutically used radionuclides such as ^{111}In and [90]Y [35–39].

Here we report the synthesis of well defined water-soluble POx, its conjugation with DOTA at the chain end and labeling of these constructs with [111]In. The *in vivo* biodistribution of this construct as well as its excretion was investigated in mice.

2. Materials and methods

2.1. Chemicals and methods

All substances were purchased from Sigma-Aldrich (Munich, Germany) and were used as received unless otherwise stated. Methyl trifluoromethylsulfonate (MeOTf), 2-methyl-2-oxazoline (MOx), 2-ethyl-2-oxazoline (EOx), acetonitrile (ACN) for polymer preparation and other solvents were dried by refluxing over CaH_2 under a dry nitrogen atmosphere and subsequent distillation prior to use. 2-(4-Isothiocyanatobenzyl)-*N,N'*, *N'',N'''*-tetraazacylododecane-1,4,7,10-tetraacetic acid×3.5 HCl (*p*-SCN-Bn-DOTA) was purchased from Macrocyclics Inc. (Dallas, TX, US) and used as received.

NMR spectra were recorded on a Bruker ARX 300 ([1]H: 300.13 MHz) or a Bruker AC 250 ([1]H: 250.13 MHz) at room temperature. The spectra were calibrated using the solvent signals ($CDCl_3$ 7.26 ppm, D_2O 4.67 ppm). Gel permeation chromatography (GPC) was performed on a Waters system (pump mod. 510, RI-detector mod. 410, precolumn PLgel and two PL Resipore columns (3 μm, 300×7.5 mm)) with *N,N*-dimethyl acetamide (DMAc) (75 mmol/L LiBr, *T*=80 °C, 1 mL/min) as eluent and calibrated against polystyrene standards. HPLC was performed on a HP1100 series with water (0.1% TFA, solvent A) and ACN (0.1% TFA, solvent B) as the mobile and Nucleosil 100 RP-18 as the stationary phase.

MALDI-TOF mass spectrometry was performed on a Bruker-Daltonic, Ultraflex TOF/TOF system using a dithranol matrix. The samples were prepared from a chloroform solution (*c*=0.5 mg/mL). Detection was made in linear as well as reflection mode. Otherwise, the sample preparation and data accumulation was performed according to [11].

2.2. Animals

Female 7–8 week old CD1 mice (Charles River, Germany) were used for *in vivo* studies. The animals were given access to food and water ad libitum. Animal studies were conducted according to the guidelines of the ethical board of the TU München.

2.3. Preparation of amine terminated poly(2-oxazoline)s

2.3.1. Poly(2-methyl-2-oxazoline)-N-tert.-butyloxycarbonylpiperazine, PMOx₄₈BocPip

PMOx₄₈BocPip was prepared by living cationic polymerization of the monomer 2-methyl-2-oxazoline (1.56 g, 18.3 mmol, 48 eq) and with 63 mg of the initiator methyl trifluoromethylsulfonate (methyl triflate, MeOTf) (0.38 mmol, 1 eq) dissolved in 10 mL acetonitrile (ACN) at 0 °C. After polymerization for 3 days at 85 °C, the reaction mixture was again cooled to 0 °C (ice bath) and 188 mg *N-tert*.-butyloxycarbonylpiperazine (*N*-Boc-piperazine) (1.0 mmol, 2.7 eq) dissolved in 750 μL ACN were added for termination of the polymerization. After stirring at room temperature (rt) for 4 h, a spatula's tip of finely ground anhydrous potassium carbonate was added. After 3 days stirring at rt the solvent was removed under reduced pressure and the residue was dissolved in 20 mL of 3:1 (v/v) mixture of chloroform and methanol (MeOH). After filtration, the polymer product was precipitated in 300 mL cold diethylether. By lyophylization, the product was obtained as a colorless solid (1.37 g, 84%). M_n(theo.)=4285 g/mol. ^{1}H NMR (D_2O, 300 MHz): δ=3.45 (br, 240H, N–CH_2–CH_2–N), 2.98/ 2.84 (br, 3H, CH_3–N), 2.00 (br, 180H, N–CO–CH_3), 1.37 ppm (s, 9H, C(CH_3)₃). GPC: M_n=6580 g/mol, PDI=1.16. HPLC: 10%B→100%B (30 min): t_r=10.2 min.

2.3.2. Poly(2-ethyl-2-oxazoline)-N-tert.-butyloxycarbonylpiperazine, PEOx$_{43}$BocPip

PEOx$_{43}$BocPip was prepared with the same procedure as described above, using 1.003 g 2-ethyl-2-oxazoline (10.1 mmol, 43 eq), 39 mg MeOTf (0.24 mmol, 1 eq) and 125 mg N-Boc-piperazine (0.67 mmol, 2.8 eq) in 9 mL ACN. The product was obtained as a colorless solid (0.94 g, 88%). M_n(theo.) = 4463 g/mol. ^{1}H NMR (CDCl$_3$, 300 MHz): δ = 3.39 (br, 222H, N–CH_2–CH_2–N), 2.96/2.90 (br, 3H, CH_3–N), 2.34 (br, 124H, N–CO–CH_2–CH$_3$), 1.39 (s, 9H, C(CH_3)$_3$), 1.06 ppm (br, 170H, N–CO–CH$_2$–CH_3). GPC: M_n = 6230 g/mol, PDI = 1.15. HPLC: 10%B → 100%B (30 min): t_r = 16.1 min.

2.3.3. Poly(2-methyl-2-oxazoline)-piperazine, PMOx$_{48}$Pip

Deprotection of the secondary amine at the chain end was performed as recently described [40]. PMOx$_{48}$BocPip (169 mg, 39 μmol) was dissolved in 1.8 mL of a 95/2.5/2.5 trifluoroacetic acid (TFA)/H$_2$O/triisobutylsilane (TIBS) (v/v/v) mixture and was left stirring for 40 min. Subsequently 2 mL MeOH and 1 mL CHCl$_3$ were added and the product was precipitated from 45 mL cold diethylether. After lyophylization 109 mg of a colorless solid was obtained (66%). M_n(theo.) = 4185 g/mol. ^{1}H NMR: (CDCl$_3$, 300 MHz): δ = 3.40 (br, 240H, N–CH_2–CH_2–N), 2.98 (br, 3H, CH_3–N), 2.08 ppm (br, 183H, N–CO–CH_3). GPC: M_n = 6360 g/mol, PDI = 1.22. HPLC: 10%B → 100%B (30 min): t_r = 9.1 min.

2.3.4. Poly(2-ethyl-2-oxazoline)-piperazine, PEOx$_{43}$Pip

Accordingly, PEOx$_{43}$BocPip (0.21 g, 47 μmol) was deprotected and the product PEOx$_{43}$Pip was obtained after lyophylization as a colorless solid (0.18 g, 88%). M_n(theo.) = 4363 g/mol. ^{1}H NMR (CDCl$_3$, 300 MHz): δ = 3.38 (br, 222H, N–CH_2–CH_2–N), 2.95/2.89 (br, 3H, CH_3–N), 2.33 (br, 121H, N–CO–CH_2–CH$_3$), 1.04 ppm (br, 168H, N–CO–CH$_2$–CH_3). GPC: M_n = 6670 g/mol, PDI = 1.18 HPLC: 10%B → 100%B (30 min): t_r = 14.8 min.

2.4. Attachment of radionuclide chelator to poly(2-oxazoline)s

2.4.1. Poly(2-methyl-2-oxazoline)-piperazine-thiouryl-p-benzyl-1,4,7,10-tetraazacyclododecane-N′,N″,N‴,N⁗-tetraacetic acid, PMOx$_{48}$PipDOTA

For preparation of PMOx$_{48}$PipDOTA, PMOx$_{48}$Pip (15 mg, 3.57 μmol, 1 eq) and 5.1 mg 2-(4-isothiocyanatobenzyl)-1,4,7,10-tetraazacyclododecane-1,4,7,10,tetraacetic acid (p-SCN-Bn-DOTA) (7.3 μmol, 2 eq) were dissolved in 500 μL MeOH and approximately 10 mg dry K$_2$CO$_3$ was added. After 3 days at rt, the solvent was removed by a stream of nitrogen. The residual was collected with 1 mL of water and the product was purified by gel filtration (Sephadex G25, 3 g). The product was obtained by lyophylization as a colorless solid (10.2 mg, 60%). M_n(theo.) = 4751 g/mol ^{1}H NMR (D$_2$O, 250 MHz): δ = 7.22/7.14 (br, 3H, Ar–H), 3.87 (br, 3H, CH_2–COOH), 3.47 (br, 223H, N–CH_2–CH_2–N^{POx}), 3.16 (br, 10H, N–CH_2–CH_2–N^{DOTA}), 2.96/2.84 (br, 3H, CH_3–N), 2.62 (br, 5H, CH_2^{Pip}), 2.00 ppm (br, 161H, N–CO–CH_3). HPLC: 10%B → 100%B (30 min): t_r = 9.2 min.

2.4.2. Poly(2-ethyl-2-oxazoline)-piperazine-thiouryl-p-benzyl-1,4,7,10-tetraazacyclododecane-N′,N″,N‴,N⁗-tetraacetic acid, PEOx$_{43}$PipDOTA

PEOx$_{43}$PipDOTA was prepared accordingly, using 15.7 mg (3.6 μmol, 1 eq) PEOx$_{43}$Pip and 5.7 mg (8.2 μmol, 2.3 eq) p-SCN-Bn-DOTA. Yield: 11 mg (62%) M_n(theo.) = 4928 g/mol. ^{1}H NMR (D$_2$O, 250 MHz): δ = 7.26/7.16 (br, 4H, Ar–H), 3.95 (br, 8H, CH_2–COOH), 3.47 (br, 232H, N–CH_2–CH_2–N^{POx}), 3.2 (br, 18H, N–CH_2–CH_2–N^{DOTA}), 3.01/2.88 (br, 3H, CH_3–N), 2.67 (br, 8H, CH_2^{Pip}), 2.32 (br, 119H, N–CO–CH_2–CH$_3$), 1.02 ppm (br, 180H, N–CO–CH$_2$–CH_3). HPLC: 10%B → 100%B (30 min): t_r = 14.5 min.

2.5. Chelation of ^{111}In to PMOx$_{48}$PipDOTA and PEOx$_{43}$PipDOTA

For chelation of ^{111}In ($t_{1/2}$ = 2.80 days) to DOTA-coupled POx, 180 μg of PMOx$_{48}$PipDOTA or PEOx$_{43}$PipDOTA were dissolved in 100 μl of 50 mM metal-free ammonium acetate buffer. 9–37 MBq of carrier-free ^{111}InCl$_3$ solution (in 0.04 M HCl, Amersham Biosciences) were added to the solution and pH was titrated to 5.0 with HCl. After an incubation period of 10 min at 65 °C, the solution was allowed to cool down at room temperature. Buffer exchange to phosphate buffered saline (PBS, pH 7.4) and elimination of unchelated ^{111}In^{3+} was performed by purification over a Sephadex G-25 spin column (illustra MicroSpin G-25 columns, GE Healthcare), which was pre-spun ten times with 350 μL PBS for 1 min at 735 g to equilibrate the column, followed by a one-minute spin at 735 g with the ^{111}In-labeled POx solution. Radiochemical purity was assessed by thin layer chromatography (silica-gel 60 F_{254} TLC aluminum sheets, Merck) using PBS containing 50 mM EDTA as the mobile phase. In this system, the R_f-values of labeled POx and unchelated ^{111}In^{3+} were found to be ∼ 0 and ∼ 0.85, respectively. The silica-gel strips were cut in the middle and radioactivity was measured in a γ-scintillation counter (1480 Wizard, Wallac). Radiochemical purity was found to be >96% after gel filtration. The labeled products were further diluted with PBS and sterile filtered prior to application in animal studies and are in the following referred to as PMOx$_{48}$PipDOTA[^{111}In] and PEOx$_{43}$PipDOTA[^{111}In], respectively.

2.6. Preparation of ^{99m}Tc-DTPA and ^{99m}Tc-MAG3

^{99m}Tc ($t_{1/2}$ = 6.01 h) was eluted from a ^{99}Mo/^{99m}Tc-generator system (Ultra-TechneKow FM, Tyco Healthcare, Germany) immediately before chelation. ^{99m}Tc-DTPA (diethylenetriaminepentaacetate, Pentacis®, Schering, Germany) and ^{99m}Tc-MAG3 (mercaptoacetyltriglycine, TechneScan® MAG3, Tyco Healthcare) were prepared using commercially available kits at the department of nuclear medicine, TU München. Radiochemical purity assessed by TLC was found to be >90%.

2.7. Biodistribution and pharmacokinetics of PMOx$_{48}$PipDOTA [^{111}In] and PEOx$_{43}$PipDOTA[^{111}In] in vivo

For biodistribution studies, 370 kBq of sterile filtered PMOx$_{48}$PipDOTA[^{111}In] or PEOx$_{43}$PipDOTA[^{111}In] diluted

with PBS were administered to each mouse in a volume of 125 µL via tail vein injection. At the indicated time points, mice were sacrificed by CO_2 asphyxia and organs were resected, weighed and assayed for accumulated radioactivity in a γ-scintillation counter. The measured activity was normalized to the sample tissue weight and to the total activity administered to the animal, while additionally performing decay correction to account for the physical half life of the radionuclide. Values are expressed as percent of injected dose per gram of tissue (%ID/g) which is proportional to the tissue concentration of the radio-labeled polymer, or as percent of injected dose (%ID) representing the accumulated amount of the radiolabeled polymer in the entire organ.

For biodistribution studies with ^{99m}Tc-DTPA and ^{99m}Tc-MAG3, each mouse was administered 3.0 MBq of the tracer diluted to 125 µL with sterile 0.9% NaCl by tail vein injection.

Table 1
Analytical data of the polymers PMOx$_{48}$BocPip and PEOx$_{43}$BocPip

Polymer	$[M]_0/[I]_0$	n^a	n^b	M^c [g/mol]	M_p^a [g/mol]	M_n^b [g/mol]	M_n^d [g/mol]	PDI^d
PMOx$_{48}$BocPip	48	49	60	4285	4370	5.3×10^3	6.6×10^3	1.16
PEOx$_{43}$BocPip	43	43	56	4463	4463	5.7×10^3	6.2×10^3	1.15

[a]Determined from MALDI-TOF MS.
[b]Determined by ^{1}H NMR end-group analysis.
[c]Calculated from $[M]_0/[I]_0$.
[d]Determined by GPC. PDI = M_w/M_n.

The further protocol for data collection and evaluation was as described above.

2.8. In vivo γ-camera imaging of PMOx$_{48}$PipDOTA[^{111}In]

7.4 MBq of PMOx$_{48}$PipDOTA[^{111}In] diluted with PBS to a final volume of 125 µL was administered by tail vein injection under sterile conditions. After 30 min and 3 h, the animal was imaged on a γ-camera (Forte, Philips Medical Systems, Germany) at ventral views under isoflurane inhalation anesthesia. Images were acquired over 1200 s on a $256 \times 256 \times 16$ (30×30 cm^2) matrix, ^{111}In flood correction was enabled, using a medium energy/general purpose (MEGP) collimator. Standards containing 10% of the injected tracer (740 kBq) diluted to 1 mL with PBS were acquired simultaneously to allow quantitative region of interest (ROI) analysis. ROIs were drawn and analyzed for the whole body, the bladder region, the standards and the background activity.

3. Results and discussion

3.1. Synthesis of the polymer carrier

The synthesis of the two hydrophilic homopolymers by living cationic polymerization of the monomers 2-methyl-2-oxazoline (MOx) and 2-ethyl-2-oxazoline (EOx) with methyl triflate (MeOTf) as the initiator and *N*-Boc-piperazine (BocPip) as the termination agent is outlined in Fig. 1. The degree of polymerization (*n*) was adjusted to result in comparable average molar mass values of around 4500 g/mol for both polymers by the initial initiator to monomer ratio ($[M]_0/[I]_0$). For PMOx$_n$ the targeted degree of polymerization was $n = 48$ and for PEOx$_n$ $n = 43$, respectively.

Both polymers were fully characterized by means of ^{1}H NMR spectroscopy, gel permeation chromatography (GPC) and MALDI-TOF mass spectrometry. The analytical data are summarized in Table 1.

For both polymers, the GPC elugrams confirmed a narrow molar mass distribution (PDI below 1.2). However, the number average molar mass values (M_n) are considerably different to the adjusted molar mass and are not confirmed by the results obtained by ^{1}H NMR end-group analysis and mass spectrometry. This discrepancy is a well-known phenomenon in the analysis of the polar poly(2-oxazoline)s with GPC due to the calibration with e.g. polystyrene standards and was discussed in detail before [10,29,41]. The end-group analysis based on the

Fig. 1. Reaction scheme for the polymerization of PMOx$_{48}$BocPip and PEOx$_{43}$BocPip as well as the consecutive polymer analogue conversions to PMOx$_{48}$PipDOTA[^{111}In] and PEOx$_{43}$PipDOTA[^{111}In].

a)

b)
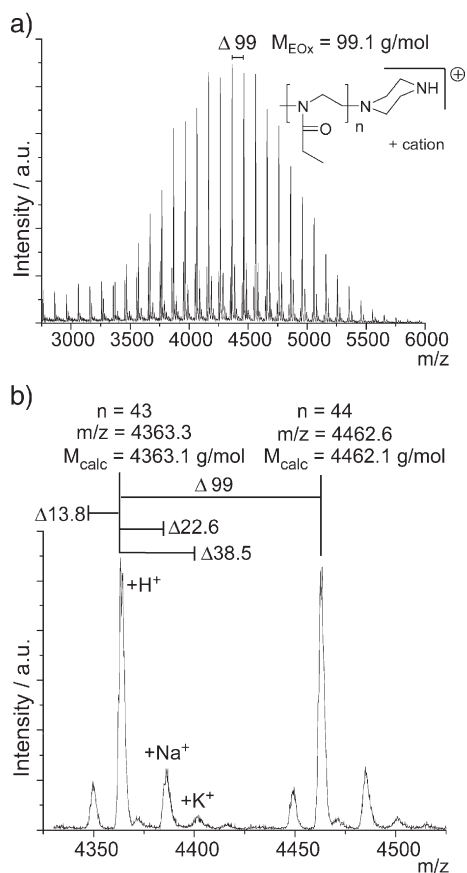
Fig. 2. MALDI-TOF mass spectrum of PEOx$_n$Pip detected in reflection mode with a mass cut-off at 1000 m/z to eliminate mass signals originating from the matrix (dithranol). a) Complete area of all mass signals originating from the polymer along with the polymer structure. b) Detail of the two most intense signal groups assigned to polymer species of n=43 and 44.

^{1}H NMR data (signals of terminal groups in relation to signals of the monomer unit. E.g. for PMOx$_{48}$BocPip signal ratio of (a) or (e) to (b) or (c) in Fig. 3a) also results in higher but again different degrees of polymerization for both polymers than expected. However, within the intrinsic error of this method caused by the low intensities for the integral values, the calculated degrees of polymerizations are in reasonable accordance with the expected ones. Since both standard analytical techniques are relative or equivalent methods for the determination of the polymer molar mass, MALDI-TOF mass spectrometry was performed for further elucidation. The direct comparison of M_p (mass of the most intense signal) of the MALDI-TOF mass spectrometry data with the values calculated from $[M]_0/[I]_0$ shows an excellent agreement (Table 1). For both polymers the mass spectra show one distribution of polymer species with mass differences matching the monomer unit mass. All detected signals could be directly assigned to positive ion species with a polymer composition of PMOx$_n$BocPip and PEOx$_n$BocPip as depicted in Fig. 1. Deprotection of the terminal secondary amine function results in PMOx$_n$Pip and PEOx$_n$Pip, which were again analyzed by MALDI-TOF mass spectrometry. Exemplary, the MALDI-TOF spectrum of PEOx$_{43}$Pip is shown in Fig. 2.

The complete mass spectrum of the deprotected polymer in Fig. 2a shows again a monomodal polymer distribution with main mass signals spaced by $\triangle m/z$=99 which is in accordance with the monomer unit mass of M_{EOx}=99.13 g/mol. Fig. 2b shows a detail around the most intense signal at m/z=4363.3. This detected species can be assigned to the cationic species [PEOx$_n$Pip+H]$^+$ with n=43 which calculates to a theoretical molar mass of M_{calc}=4363.1 g/mol. Accordingly, signals within

a)

b)

c)
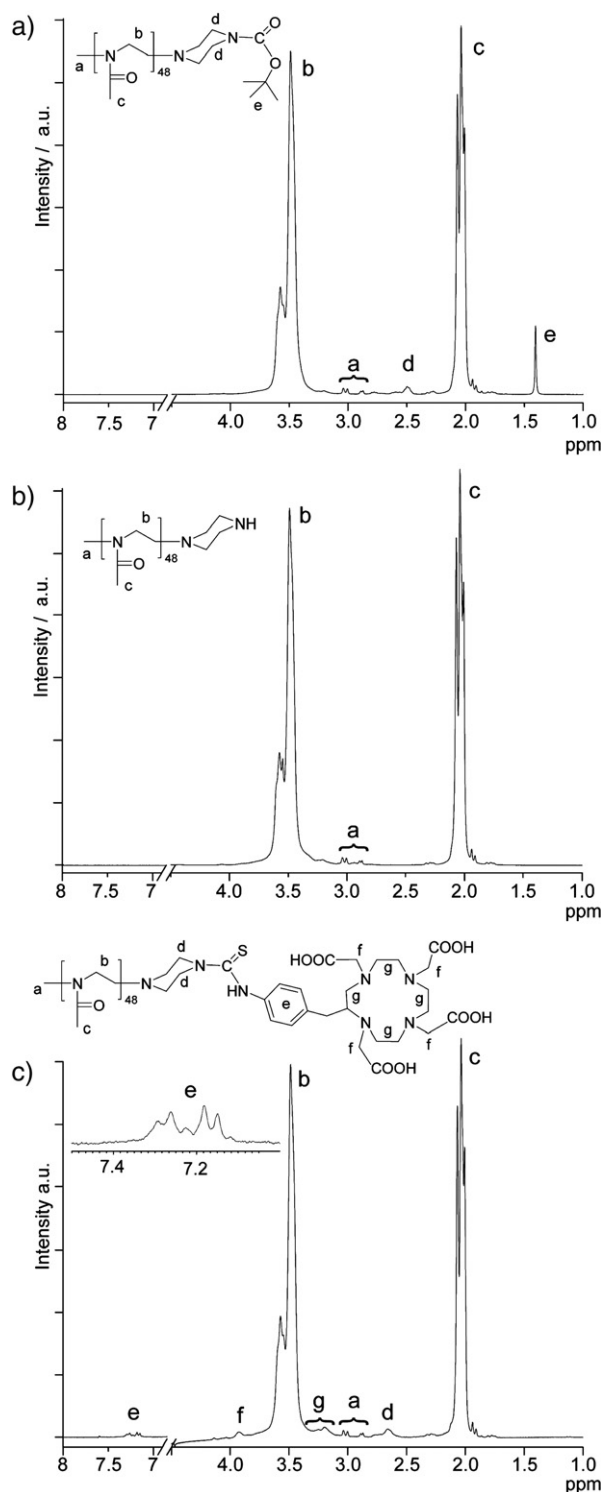
Fig. 3. ^{1}H NMR spectra of a) PMOx$_{48}$BocPip, b) the deprotected PMOx$_{48}$Pip and c) the chelator functionalized PMOx$_{48}$PipDOTA along with the respective structures and assignments. The spectra were recorded at 250 MHz in D$_2$O.

Table 2
Biodistribution of PMOx$_{48}$PipDOTA[^{111}In]

	30 min	3 h	24 h
Blood	0.637±0.121	0.228±0.026	0.077±0.022
Heart	0.192±0.048	0.075±0.016	0.056±0.006
Lungs	0.443±0.046	0.230±0.077	0.137±0.014
*Kidneys	1.526±0.132	1.114±0.098	0.964±0.170
Liver	0.165±0.036	0.118±0.014	0.136±0.026
Spleen	0.147±0.037	0.091±0.030	0.125±0.025
Pancreas	0.139±0.022	0.068±0.003	0.060±0.007
Muscle	0.121±0.050	0.032±0.006	0.027±0.004
Skin	0.362±0.138	0.081±0.014	0.070±0.012
Fat tissue	0.054±0.009	0.025±0.002	0.017±0.007
Stomach	0.234±0.066	0.071±0.012	0.059±0.007
Jejunum	0.147±0.034	0.068±0.026	0.108±0.015
Colon	0.192±0.041	0.073±0.022	0.094±0.014
Bone with marrow	0.110±0.011	0.093±0.009	0.109±0.049
Brain	0.020±0.002	0.013±0.003	0.010±0.003

All values are means of %ID/g±SD (n=3).
*n=6.

this main population can be assigned for chain length between n=28 (m/z=2875.9; M(PEOx$_{28}$Pip)=2875.0 g/mol) and n=58 (m/z=5852.0; M(PEOx$_{58}$Pip)=5849.8).

The main signals are accompanied by smaller signals with $\triangle m/z$=22.6 and 38.5 which are assignable to the cationic species [PEOx$_{43}$Pip+Na]$^{+}$ and [PEOx$_{43}$Pip+K]$^{+}$ respectively. Furthermore, a third minor species with a lower mass relative to the main population at $\triangle m/z$=14 was detected. For MALDI-TOF spectra of poly(2-ethyl-2-oxazoline)s this has been observed earlier [11] and can be attributed to fragmentation of a methyl group and recombination with a hydrogen during the measurement or by an initiation reaction of a small fraction of monomers with a proton instead of the initiator MeOTf. However, the intensity of this subpopulation is low and the molar mass of the resulting polymer is not significantly affected. Taking all signals and their respective intensities into account, a M_{n} and M_{w} of PEOx$_{43}$Pip based on the mass spectrometry was calculated to be M_{n}=4151.9 g/mol and M_{w}=4282.4 g/mol giving a very narrow polydispersity index of 1.03.

Similar results were found for PMOx$_{48}$Pip, although the mass spectrum showed that the mass distribution showed a slightly larger fraction of low molar mass species. At this point it can be concluded that the living cationic polymerization of MOx and EOx resulted in structurally defined polymers of the desired length with a very narrow molar mass distribution. Moreover, the end functionality N-Boc-piperazine was quantitatively introduced by the termination reaction and could be quantitatively deprotected as confirmed by MALDI-TOF mass spectrometry.

In addition the polymer analog reactions, deprotection of the terminal piperazine and the functionalization of the polymer with p-SCN-Bn-DOTA were followed by HPLC and ^{1}H NMR spectroscopy (Fig. 3).

In agreement with the mass spectrometry results, the structure of PMOx$_{48}$BocPip was confirmed by ^{1}H NMR spectroscopy. The presence of the terminal methyl group introduced by the initiation reaction as well as the Boc-protected piperazine

introduced by the termination reaction is confirmed by the signals (a) around 3.0 ppm and (d, e) at 2.5 and 1.37 ppm, respectively (Fig. 3a). The absence of the *tert.*-butyl signals (e) in the spectrum shown in Fig. 3b, shows the successful and quantitative deprotection of the second amine group of the piperazine. The final functionalization of the polymer with the DOTA chelator by the reaction of the isothiocyanate with the secondary amine group of the terminal piperazine was proven by the appearance of the additional signals of the aromatic linker (e at 7.2 ppm), the methylene signals of the DOTA ring structure (g at 3.2 ppm) and the methylene group of the attached acetic acid function (f at 3.9 ppm) in the spectrum in Fig. 3c. The integral signal ratios suggest a near quantitative coupling in the case of PEOx$_{43}$PipDOTA and approximately 85% reaction yield for PMOx$_{48}$PipDOTA. Although NMR integrals have to be interpreted with care, it can already be stated that the DOTA was attached to the polymer with good efficiency. An analog series of spectra were obtained for the PEOx$_{43}$ polymer (not shown, see the experimental part for details).

These data were corroborated by HPLC analysis. Deprotection of PMOx$_{48}$BocPip resulted in a shift of the elution peak of ~1 min and no signal was detected at the original elution time of the educt. In the same manner the subsequent coupling with p-SCN-Bn-DOTA could be easily followed with HPLC. Although the retention time did not shift significantly upon the coupling reaction, it was confirmed by the additional absorption at 254 nm, coappearing with the broad polymer signal at 220 nm, which was absent in the unmodified polymer. Since in no case neither a second elution peak nor a broadening of the polymer peak was observed, the HPLC results suggest that the polymer analog reactions were quantitative to the final polymer compounds PMOx$_{48}$PipDOTA and PEOx$_{43}$PipDOTA.

In a final step, both polymers were radiolabeled with ^{111}In by chelation to the polymer-linked DOTA moiety. Using thin layer chromatography in combination with a γ-scintillation counter, the radiochemical purity of both polymers was found to be >96%.

Table 3
Biodistribution of PEOx$_{43}$PipDOTA[^{111}In]

	30 min	3 h	24 h
Blood	1.267±0.014	0.368±0.023	0.085±0.008
Heart	0.325±0.022	0.125±0.020	0.071±0.005
Lungs	0.731±0.111	0.278±0.110	0.114±0.006
*Kidneys	3.643±0.225	2.394±0.147	2.380±0.217
Liver	0.312±0.019	0.193±0.013	0.274±0.026
Spleen	0.198±0.032	0.132±0.005	0.155±0.062
Pancreas	0.211±0.040	0.101±0.021	0.103±0.016
Muscle	0.183±0.009	0.055±0.005	0.043±0.014
Skin	0.927±0.176	0.185±0.028	0.192±0.043
Fat tissue	0.146±0.023	0.041±0.009	0.059±0.007
Stomach	0.318±0.018	0.094±0.016	0.086±0.007
Jejunum	0.260±0.050	0.097±0.015	0.154±0.025
Colon	0.291±0.027	0.091±0.019	0.142±0.043
Bone with marrow	0.495±0.094	0.222±0.034	0.353±0.132
Brain	0.049±0.009	0.015±0.002	0.007±0.001

All values are means of %ID/g±SD (n=3).
*n=6.

3.2. Biodistribution and pharmacokinetics of PMOx$_{48}$PipDOTA [^{111}In] and PEOx$_{43}$PipDOTA[^{111}In] in vivo

The measured radioactivity concentrations of PMOx$_{48}$PipDOTA [^{111}In] and PEOx$_{43}$PipDOTA[^{111}In], expressed as percent of injected dose per gram of tissue (%ID/g), which are proportional to the POx concentrations, are summarized in Tables 2 and 3.

The highest tracer concentrations were found in the kidneys, most likely due to secretion of the polymers. No significant accumulation of polyoxazolines was found in all tissues tested as the measured activity concentrations corresponded to a normal blood pool distribution. The lowest tissue concentration was found in the brain, indicating that these poly(2-oxazoline)s do not cross the blood–brain barrier.

The slight increase of radioactivity in the liver, spleen and bone with marrow from 3 h to 24 h may indicate a small uptake of PMOx and PEOx by the RES. The total accumulated activity in liver and spleen together, the organs representing a high fraction of the RES, was <0.2%ID of PMOx$_{48}$PipDOTA[^{111}In] and <0.4%ID of PEOx$_{43}$PipDOTA[^{111}In] 24 h post injection. This indicates that the uptake by the RES is almost negligible. Accordingly, there was no visible uptake by the liver or spleen in the images obtained by the γ-camera, see Section 3.4 and Fig. 6.

3.3. Excretion of the poly(2-oxazoline)s PMOx$_{48}$PipDOTA [^{111}In] and PEOx$_{43}$PipDOTA[^{111}In]

Intravenously injected polyoxazolines were quickly eliminated from the blood (Fig. 4). Only about 2%ID and 0.8%ID of PMOx$_{48}$PipDOTA[^{111}In] remained in the total blood pool at 30 min and 3 h after tracer injection, respectively. For PEOx$_{43}$PipDOTA[^{111}In], these fractions were 4%ID at 30 min and 1%ID at 3 h. Tracer excretion proceeded slightly slower after this time period, with about 0.2–0.3%ID remaining in the total blood pool 24 h post injection. In the kidneys peak values were measured 30 min after injection with 1.5%ID/g and 3.6% ID/g for PMOx$_{48}$PipDOTA[^{111}In] and PEOx$_{43}$PipDOTA
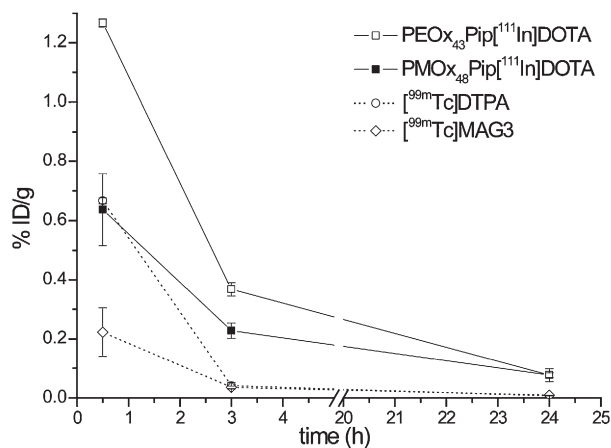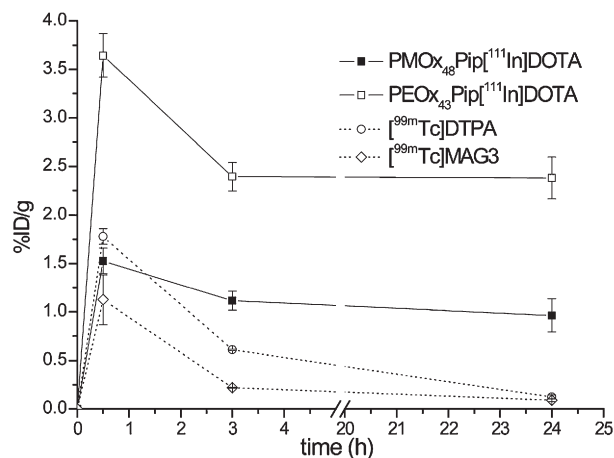
Fig. 5. Comparison of kidney uptake of ^{111}In-labeled POx with ^{99m}Tc-DTPA and ^{99m}Tc-MAG3.

[^{111}In], respectively (Fig. 5). This corresponds to a total accumulated activity per kidney of 0.4%ID for PMOx and 0.6%ID for PEOx at 30 min post injection.

These findings suggest that PMOx and PEOx are predominantly excreted via the kidneys. To further characterize the mechanism of renal excretion, we compared the rates of blood clearance of POx with ^{99m}Tc-diethylenetriaminepentaacetate (DTPA) and ^{99m}Tc-mercaptoacetyltriglycine (MAG3) (Tables 4a and b, Fig. 4). These two tracers are widely used in nuclear medicine to assess kidney function and have already been extensively evaluated [42–46]. DTPA is excreted exclusively by complete renal glomerular filtration, but is neither secreted nor reabsorbed in the renal tubuli. Thus, the rate of blood clearance of DTPA corresponds to the glomerular filtration rate. In contrast, MAG3 is partly excreted by glomerular filtration and is additionally secreted by the tubuli almost completely, resulting in a blood clearance rate nearly corresponding to the renal plasma flow. As the tested polymers are uncharged (apart from the DOTA moiety) and have a molar mass of about 5 kDa, comparable to inulin, we assumed that these tracers would be, like DTPA, freely filtrated in the glomerulus. As expected, the blood clearance rates of ^{111}In-labeled POx are high, but are still significantly lower than those of DTPA and MAG3. This might indicate that a small fraction of POx binds to plasma proteins and is thus not accessible to filtration in the glomerulus. This assumption is supported by the finding that the blood clearance of PEOx$_{43}$PipDOTA[^{111}In] is slower compared to PMOx$_{48}$ PipDOTA[^{111}In] which can be explained by the more amphiphilic nature of the ethyl residues of PEOx, compared to the methyl residues of PMOx. The higher amphiphilicity could cause a higher binding affinity of PEOx to e.g. plasma proteins

Fig. 4. Comparison of blood pool clearance of ^{111}In-labeled POx with ^{99m}Tc-DTPA (glomerular filtration) and ^{99m}Tc-MAG3 (tubular secretion).

Table 4a
Biodistribution of ^{99m}Tc-DTPA

	30 min	3 h	24 h
Blood (n=3)	0.667±0.010	0.041±0.011	0.007±0.0002
Kidneys (n=6)	1.778±0.080	0.609±0.063	0.123±0.0210

All values are means of %ID/g±SD.

Table 4b
Biodistribution of ^{99m}Tc-MAG3

	30 min	3 h	24 h
Blood ($n=3$)	0.223±0.082	0.036±0.004	0.009±0.0005
Kidneys ($n=6$)	1.126±0.257	0.218±0.036	0.090±0.0144

All values are means of %ID/g±SD.

that could result in a lower fraction of filtration in the kidney as compared to the hydrophilic PMOx. The observation that the activity in the kidney does not show a further washout after 3 h post injection might indicate an uptake and trapping of small amounts of tracer into the renal tubular cells.

Elimination of POx by hepatobiliary excretion seems to play only a minor role. Only a very low accumulation of tracer can be seen in the hepatobiliary tract, but the observation of an increase of radioactivity between 3 h and 24 h in the liver, jejunum and colon, but not in the stomach, points to a minute hepatobiliary excretion of POx.

3.4. Scintigraphic imaging of ^{111}In-labeled polyoxazolines in vivo

In vivo imaging studies were performed 30 min and 3 h after intravenous administration of PMOx$_{48}$PipDOTA[^{111}In]. Both images obtained are shown in Fig. 6. Areas with notable higher tracer accumulation are the bladder, the kidneys and the blood pool in the heart. The remaining tracer activity is distributed homogeneously over the body with no further significant tracer accumulation. Significant lower total body activity is visible at 3 h compared to the 30 min image. ROI analysis added up to a remaining total body activity (excluding bladder activity) of 11%ID at 30 min and 4.5%ID at 3 h after tracer injection.

3.5. Biodistribution of POx compared to previous studies

Biodistribution studies with POx have already been conducted, using ^{125}I-labeled POx-conjugates with a molecular weight of 15 kDa and 29 kDa (polyethylene glycol) GPC calibration; 45 kDa and 120 kDa when calibrated against poly [N-(2-hydroxypropyl)methacrylamide] poly(HPMA), all values M_w) [6]. The reported blood clearance of these constructs was significantly slower compared to the constructs described by us, as about 7% (15 kDa polymer) and 28% (29 kDa polymer) of the injected dose were present in the blood pool 24 h after injection. These findings can be explained by the higher molecular weight of the polymers used, resulting in a lower glomerular filtration fraction. The uptake of these constructs by the RES was significantly higher than the uptake of the polymers tested in our study. Moreover, significant tracer accumulation in the skin and muscle tissue was reported in this study, whereas we did not find accumulation in these tissues. These results indicate that the low molecular weight polymers described by us are more appropriate for medical use in radionuclide therapy.

3.6. Biodistribution of POx compared to HPMA and PEG

N-(2-hydroxypropyl)-methacrylamide (HPMA) copolymers have been conjugated with a variety of molecules and are being studied as promising drug carriers for tumor therapy, either using the unspecific enhanced permeability and retention (EPR) effect or specific targeting molecules to increase tumor uptake and reduce side effects [2,47–50]. Biodistribution studies of ^{99m}Tc-labeled HPMA copolymers of different molecular weights and charge have already been conducted in SCID mice [51]. A neutral 7 kDa (M_w) ^{99m}Tc-HPMA copolymer fraction, comparable to the neutral 5 kDa POx presented in our study, displayed a clearly higher blood pool activity (13 times), higher kidney uptake (1.5–4 times) and more activity in the spleen and liver (19–47 times) 24 h post injection, showing slower excretion and indicating higher uptake by the RES. A negatively charged variant of the 7 kDa HPMA copolymer was excreted faster and uptake by spleen and liver was reduced significantly, blood pool, spleen and liver uptake were comparable to POx, whereas kidney uptake was still significantly higher (3.5–8.5 times). This suggests that functionalized POx may be better suitable for targeted therapy of tumors than HPMA copolymers. However, it is important to keep in mind that the molar mass, as determined by GPC strongly depends on the used mobile phase and the calibration. This has to be considered for the comparison of biodistribution results for polymers of different analytical background.

Whereas our intended use for radiolabeled POx is multiple functionalization of the side chains to increase the avidity of tumor-targeting molecules while maintaining rapid blood clearance to minimize radiation exposure of the patient, the medical use of PEG-based polymers is based on another approach, as it is difficult to introduce multiple functionalities into these polymers. They are mainly used to PEGylate biological active molecules to alter their immunogenicity and pharmacokinetics like protection from degradation, increased water solubility and reduced renal excretion [2,3]. In contrast, POx are well-known to be
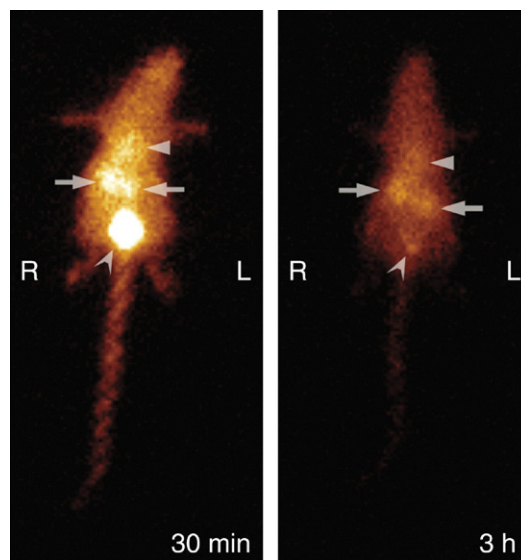
Fig. 6. γ-camera imaging of in vivo distribution of PMOx$_{48}$PipDOTA[^{111}In] in a CD1 mouse 30 min and 3 h after intravenous injection. Areas with highest activity concentration are the bladder (thin arrowhead), the kidneys (arrows) and the blood pool in the heart (thick arrowhead).

functionalizable at the side chains by a number of different efficient coupling methods, including thioisocyanate coupling [34,52], ester and amide formation [53,54], oxime formation [33] and click chemistry [10]. Moreover, PEG-polymers are present in the circulation for longer times compared to hydrophilic poly(2-alkyl-2-oxazoline)s. ^{14}C-labeled PEG with an average molar mass of 4000 g/mol showed an excretion of 93.2% one day after intravenous injection [55], whereas ROI analysis showed that PMOx$_{48}$PipDOTA[^{111}In] was excreted by 95.5% already 3 h after administration (see Section 3.4). The slower excretion would increase side effects in radionuclide therapy as the effective half life of the radionuclides administered would be longer, resulting in a higher radiation exposure of the patient. Therefore, hydrophilic poly(2-oxazoline)s may turn out to be more effective carriers in radionuclide therapy in the future.

4. Conclusion

Water-soluble poly(2-oxazoline)s fulfill all requirements for carrier molecules in radionuclide therapy and tumor imaging. Here we report the synthesis of chemically well defined, water-soluble DOTA-PMOx and DOTA-PEOx conjugates, labeling of the polymers with ^{111}In and their application for *in vivo* imaging studies. The radiolabeled PMOx$_{48}$PipDOTA[^{111}In] and PEOx$_{43}$PipDOTA[^{111}In] are rapidly cleared from the blood pool, predominantly by renal glomerular filtration and do not accumulate in body tissues, thus minimizing radiation exposure of the patient. The uptake into the RES is minimal. In the future, DOTA-coupled poly(2-oxazoline)s can be conjugated with multiple functionalities such as tumor-targeting peptides via functional monomer units and therapeutically active radionuclides such as [90]Y. Further studies are justified to generate and to test these polymers and related work is currently in progress in our laboratories.

Acknowledgements

References

[1] H. Ringsdorf, Structures and properties of pharmacologically active polymers, J. Polym. Sci., Polym. Symp. 51 (1975) 135–153.

[2] R. Duncan, The dawning era of polymer therapeutics, Nat. Rev. Drug Discov. 2 (2003) 347–360.

[3] G. Pasut, F.M. Veronese, PEGylation of proteins as tailored chemistry for optimized bioconjugates, Adv. Polym. Sci. 192 (2005) 95–134.

[4] R. Haag, F. Kratz, Polymer therapeutics: concepts and applications, Angew. Chem., Int. Ed. 45 (2006) 1198–1215.

[5] H. Frey, R. Haag, Dendritic polyglycerol: a new versatile biocompatible material, Rev. Mol. Biotechnol. 90 (2002) 257–267.

[6] P. Goddard, L.E. Hutchinson, J. Brown, L.J. Brookman, Soluble polymeric carriers for drug delivery. Part 2. Preparation and in vivo behaviour of *N*-acylethylenimine copolymers, J. Control. Release 10 (1989) 5–16.

[7] S. Zalipsky, C.B. Hansen, J.M. Oaks, T.M. Allen, Evaluation of blood clearance rates and biodistribution of poly(2-oxazoline)-grafted liposomes, J. Pharm. Sci. 85 (2) (1996) 133–137.

[8] S.C. Lee, C. Kim, I.C. Kwon, H. Chung, S.Y. Jeong, Polymeric micelles of poly(2-ethyl-2-oxazoline)-block-poly(ε-caprolactone) copolymer as a carrier for paclitaxel, J. Control. Release 89 (2003) 437–446.

[9] M.C. Woodle, C.M. Engbers, S. Zalipsky, New amphipatic polymer-lipid conjugates forming long-circulating reticuloendothelial system-evading liposomes, Bioconjug. Chem. 5 (1994) 493–496.

[10] R. Luxenhofer, R. Jordan, Click chemistry with poly(2-oxazoline)s, Macromolecules 39 (10) (2006) 3509–3516.

[11] R. Jordan, K. Martin, H.J. Räder, K.K. Unger, Lipopolymers for surface functionalizations. 1. Synthesis and Characterization of terminal functionalized poly(*N*-propionylethylenimine)s, Macromolecules 34 (26) (2001) 8858–8865.

[12] S. Kobayashi, H. Uyama, N. Higuchi, T. Saegusa, Synthesis of a nonionic polymer surfactant from cyclic imino ethers by the terminator method, Macromolecules 23 (1) (1990) 54–59.

[13] D. Christova, R. Velichkova, E.J. Goethals, Bis-macromonomers of 2-alkyl-2-oxazolines-synthesis and polymerization, Macromol. Rapid Commun. 18 (12) (1997) 1067–1073.

[14] S. Kobayashi, E. Masuda, S.-I. Shoda, Y. Shimano, Synthesis of acryl- and methacryl-type macromonomers and telechelics by utilizing living polymerization of 2-oxazolines, Macromolecules 22 (7) (1989) 2878–2884.

[15] O. Nuyken, G. Maier, A. Gro, H. Fischer, Systematic investigations on the reactivity of oxazolinium salts, Macromol. Chem. Phys. 197 (1) (1996) 83–95.

[16] M. Miyamoto, K. Naka, M. Tokumizu, T. Saegusa, End capping of growing species of poly(2-oxazoline) with carboxylic acid: a novel and convenient route to prepare vinyl- and carboxy-terminated macromonomers, Macromolecules 22 (4) (1989) 1604–1607.

[17] S. Kobayashi, S. Iijima, T. Igarashi, T. Saegusa, Synthesis of a nonionic polymer surfactant from cyclic imino ethers by the initiator method, Macromolecules 20 (8) (1987) 1729–1734.

[18] M. Einzmann, W.H. Binder, Novel functional initiators for oxazoline polymerization, J. Polym. Sci., A, Polym. Chem. 39 (16) (2001) 2821–2831.

[19] R. Jordan, A. Ulman, Surface initiated living cationic polymerization of 2-oxazolines, J. Am. Chem. Soc. 120 (2) (1998) 243–247.

[20] R. Jordan, N. West, A. Ulman, Y.-M. Chou, O. Nuyken, Nanocomposites by surface-initiated living cationic polymerization of 2-oxazolines on functionalized gold nanoparticles, Macromolecules 34 (6) (2001) 1606–1611.

[21] Y. Chujo, E. Ihara, H. Ihara, T. Saegusa, A novel silane coupling agent. 1. Synthesis of trimethoxysilyl-terminated poly(*N*-acetylethylenimine), Macromolecules 22 (5) (1989) 2040–2043.

[22] S. Kobayashi, H. Uyama, Synthesis of a nonionic polymeric surfactant from 2-oxazolines having a carboxylate component as the hydrophobic group, Macromolecules 24 (19) (1991) 5473–5475.

[23] A. Levy, M. Litt, Polymerization of cyclic iminoethers. V. 1,3-Oxazolines with hydroxy-, acetoxy-, and carboxymethyl-alkyl groups in the 2 position and their polymers, J. Polym. Sci., A, Polym. Chem. 6 (1968) 1883–1894.

[24] J.O. Krause, M.T. Zarka, U. Anders, R. Weberskirch, O. Nuyken, M.R. Buchmeiser, Simple synthesis of poly(acetylene) latex particles in aqueous media, Angew. Chem., Int. Ed. 42 (2003) 5965–5969.

[25] G. Odian, F. Shi, Thermal polymerization of hydroxy- and mercapto-substituted 2-oxazolines, Macromolecules 26 (1993) 17–23.

[26] M.T. Zarka, O. Nuyken, R. Weberskirch, Amphiphilic polymer supports for the asymmetric hydrogenation of amino acid precursors in water, Chem.-Eur. J. 9 (2004) 3228–3234.

[27] B.R. Hsieh, M.H. Litt, Poly(*N*-acylethylenimines) with pendant carbazole derivatives. 1. Synthesis, Macromolecules 18 (1985) 1388–1394.

[28] B.R. Hsieh, M.H. Litt, Poly(*N*-acylethylenimines) with pendant carbazole derivatives. 2. Synthesis of 3,6-dimethoxy-, 3,6-dihydroxy-, and 2,7-dihydroxycarbazole-containing polymers, Macromolecules 19 (1986) 516–520.

[29] P. Persigehl, R. Jordan, O. Nuyken, Functionalization of amphiphilic poly (2-oxazoline) block copolymers: a novel class of macroligands for micellar catalysis, Macromolecules 33 (2000) 6977–6981.

[30] Y. Chujo, K. Sada, T. Saegusa, Iron(II) bipyridyl-branched polyoxazoline complex as a thermally reversible hydrogel, Macromolecules 26 (1993) 6315–6319.

[31] T. Kotre, O. Nuyken, R. Weberskirch, ATRP of MMA in aqueous solution in the presence of an amphiphilic polymeric macroligand, Macromol. Rapid Commun. 23 (2002) 871–876.

[32] Y. Chujo, K. Sada, T. Saegusa, Reversible gelation of polyoxazoline by means of Diels–Alder reaction, Macromolecules 23 (1990) 2636–2641.

[33] C. Taubmann, R. Luxenhofer, S. Cesana, R. Jordan, First aldehyde-functionalized poly(2-oxazoline)s for chemoselective ligation, Macromol. Biosci. 5 (7) (2005) 603–612.

[34] S. Cesana, J. Auernheimer, R. Jordan, H. Kessler, O. Nuyken, First poly(2-oxazoline)s with pendant amino groups, Macromol. Chem. Phys. 207 (2006) 183–192.

[35] S. Liu, D.S. Edwards, Bifunctional chelators for therapeutic lanthanide radiopharmaceuticals, Bioconjug. Chem. 12 (1) (2001) 7–34.

[36] D.J. Kwekkeboom, W.H. Bakker, B.L. Kam, J.J.M. Teunissen, P.P.M. Kooij, W.W. Herder, R.A. Feelders, C.H.J. Eijck, M. de Jong, A. Srinivasan, J.L. Erion, E.P. Krenning, Treatment of patients with gastro-entero-pancreatic (GEP) tumors with the novel radiolabeled somatostatin analogue [^{177}Lu–DOTA^0,Tyr^3]octreotate, Eur. J. Nucl. Med. Mol. Imaging 30 (3) (2003) 417–422.

[37] D.J. Kwekkeboom, J. Mueller-Brand, B. Paganelli, L.B. Anthony, S. Pauwels, L.K. Kvols, T.M. O'Dorisio, R. Valkema, L. Bodei, M. Chinol, H.R. Maecke, E.P. Krenning, Overview of results of peptide receptor radionuclide therapy with 3 radiolabeled somatostatin analogs, J. Nucl. Med. 46 (1) (2005) 62S–66S.

[38] X. Chen, Y. Hou, M. Tohme, R. Park, V. Khankaldyyan, I. Gonzales-Gomez, J.R. Bading, W.E. Laug, P.S. Conti, Pegylated Arg–Gly–Asp peptide: ^{64}Cu labeling and PET imaging of brain tumor $\alpha_v\beta_3$-integrin, J. Nucl. Med. 14 (10) (2004) 1776–1783.

[39] S. Koukouraki, L.G. Strauss, V. Georgoulias, J. Schuhmacher, U. Haberkom, N. Karkavitsas, A. Dimitrakopoulou-Strauss, Evaluation of the pharmacokinetics of 68-Ga–DOTATOC in patients with metastatic neuroendocrine tumors scheduled for 90Y–DOTATOC therapy, Eur. J. Nucl. Med. Mol. Imaging 33 (4) (2006) 460–466.

[40] R. Luxenhofer, M. López-García, A. Frank, H. Kessler, R. Jordan, First poly(2-oxazoline)-peptide conjugate for targeted radionuclide cancer therapy, PMSE Prepr. 95 (2006) 283–284.

[41] O. Purrucker, A. Förtig, R. Jordan, M. Tanaka, Supported membranes with well-defined polymer tethers — incorporation of cell receptors, Chem. Phys. Chem. 5 (2004) 327–335.

[42] G.L. Barbour, C.K. Crumb, C.M. Boyd, R.D. Reeves, S.P. Rastogi, R.M. Patterson, Comparison of inulin, iothalamate, and 99m-Tc-DTPA for measurement of glomerular filtration rate, J. Nucl. Med. 17 (1976) 317–320.

[43] A.R. Fritzberg, S. Kasina, D. Eshima, D.L. Johnson, synthesis and biological evaluation of technetium-99m MAG3 as a hippuran replace-ment, J. Nucl. Med. 27 (1986) 111–116.

[44] A. Taylor, D. Eshima, N. Alazraki, 99mTc-MAG3, a new renal imaging agent: Preliminary results in patients, Eur. J. Nucl. Med. 12 (1987) 510–514.

[45] A.A. Al-Nahhas, R.A. Jafri, K.E. Britton, K. Solanki, J. Bomanji, S. Mather, M.A. Carroll, M. Al-Janabi, V. Frusciante, B. Ajdinowic, F. Fiore, S. Denema, C.C. Nimmon, Clinical experience with 99mTc-MAG3, mercaptoacetyltriglycine, and a comparison with 99mTc-DTPA, Eur. J. Nucl. Med. 14 (1988) 453–462.

[46] R.A. Jafri, K.E. Britton, C.C. Nimmon, K. Solanki, A. Al-Nahhas, J. Bomanji, J. Fettich, L.A. Hawkins, Technetium-99m MAG3, a comparison with iodine-123 and iodine-131 orthoiodohippurate, in patients with renal disorders, J. Nucl. Med. 29 (1988) 147–158.

[47] A. Mitra, J. Mulholland, A. Nan, Targeting tumor angiogenic vasculature using polymer-RGD conjugates, J. Control. Release 102 (2005) 191–201.

[48] J. Kopeček, P. Kopečková, T. Minko, HPMA copolymer-anticancer drug conjugates: design, activity, and mechanism of action, Eur. J. Pharm. Biopharm. 50 (2000) 61–81.

[49] T. Lammers, R. Kühnlein, M. Kissel, V. Subr, T. Etrych, R. Pola, M. Pechar, K. Ulbrich, G. Strom, P. Huber, P. Peschke, Effect of physicochemical modification on the biodistribution and tumor accumulation of HPMA copolymers, J. Control. Release 119 (2005) 103–118.

[50] B.R. Line, A. Mitra, A. Nan, H. Ghandehari, Targeting tumor angiogenesis: comparison of peptide and polymer–peptide conjugates, J. Nucl. Med. 46 (2005) 1552–1560.

[51] A. Mitra, A. Nan, H. Ghandehari, Technetium-99m-labeled *N*-(2-hydroxypropyl) methacrylamide copolymers: synthesis, characterization, and *in vivo* biodistribution, Pharm. Res. 21 (2004) 1153–1159.

[52] T.B. Bonné, K. Lüdtke, R. Jordan, P. Stepánek, C.M. Papadakis, Aggregation behavior of amphiphilic poly(2-alkyl-2-oxazoline) diblock copolymers in aqueous solution studied by fluorescence correlation spectroscopy, Colloid Polym. Sci. 282 (2004) 833–843.

[53] B.M. Rossbach, K. Leopold, R. Weberskirch, Self-assembled nanoreactors as highly active catalysts in the hydrolytic kinetic resolution (HKR) of epoxides in water, Angew. Chem., Int. Ed. 45 (2006) 1309–1312.

[54] M.T. Zarka, O. Nuyken, R. Weberskirch, Amphiphilic polymer supports for the asymmetric hydrogenation of amino acid precursors in water, Chem.-Eur. J. 9 (2003) 3228–3234.

[55] Y. Furuichi, T. Takahashi, K. Imaizumi, M. Sugano, Evaluation of polyethylene glycol as a water-soluble marker: absorption and excretion of ^{14}C-labeled polyethylene glycol in rats, Agric. Biol. Chem. 7 (1984) 1777–1781.